Advanced Structured Materials

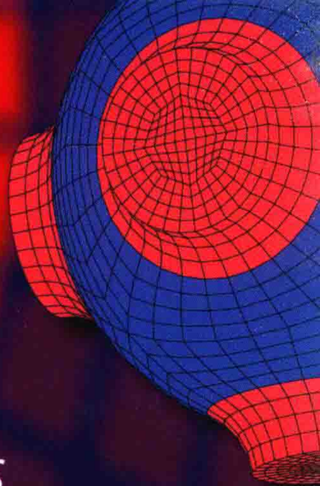

J. M. P. Q. Delgado
A. G. Barbosa de Lima *Editors*

Transport Phenomena and Drying of Solids and Particulate Materials

Springer

J. M. P. Q. Delgado · A. G. Barbosa de Lima
Editors

Transport Phenomena and Drying of Solids and Particulate Materials

Springer

Editors
J. M. P. Q. Delgado
Laboratory of Building Physics
Department of Civil Engineering
Faculty of Engineering of University of Porto
Porto
Portugal

A. G. Barbosa de Lima
Department of Mechanical Engineering
Federal University of Campina Grande
Campina Grande
Brazil

ISSN 1869-8433 ISSN 1869-8441 (electronic)
ISBN 978-3-319-04053-0 ISBN 978-3-319-04054-7 (eBook)
DOI 10.1007/978-3-319-04054-7
Springer Cham Heidelberg New York Dordrecht London

Library of Congress Control Number: 2014942711

Printed on acid-free paper

Springer is part of Springer Science+Business Media (www.springer.com)

Advanced Structured Materials

Volume 48

Series editors

Andreas Öchsner, Southport Queensland, Australia
Lucas F. M. da Silva, Porto, Portugal
Holm Altenbach, Magdeburg, Germany

For further volumes:
http://www.springer.com/series/8611

Contents

Porous Materials Drying Model Based on the Thermodynamics of Irreversible Processes: Background and Application

A. G. Barbosa de Lima, J. M. P. Q. Delgado, V. A. B. de Oliveira, J. C. S. de Melo and C. Joaquina e Silva

Abstract This chapter focuses on the heat and mass transfer (drying) in capillary-porous bodies using both the mechanistic and non-equilibrium thermodynamic approaches. A new coupled mathematical modeling to predict heat and moisture (liquid and vapor) transfer in wet capillary-porous bodies with particular reference to prolate spheroidal solids is presented and discussed. The mathematical model is based on the thermodynamics of irreversible processes by considering variable transport coefficients and equilibrium or convective boundary conditions at the surface of the solid. All the partial differential equations presented in the model have been written in prolate spheroidal coordinates. The finite-volume method has been used to obtain the numerical solution of the governing equations. Application has been done to wheat kernel drying and comparison between predicted and experimental data has showed good agreement.

Keywords Drying · Numerical solution · Mass · Heat · Elliptical geometry

---

A. G. Barbosa de Lima (✉) · J. C. S. de Melo · C. Joaquina e Silva
Department of Mechanical Engineering, Federal University of Campina Grande,
Av. Aprígio Veloso, 882 Bodocongó, Campina Grande, PB Zip Code: 58429-900, Brazil
e-mail: gilson@dem.ufcg.edu.br

J. C. S. de Melo
e-mail: jcarlosmequi@yahoo.com.br

C. Joaquina e Silva
e-mail: carlota.jsilva@gmail.com

J. M. P. Q. Delgado
LFC – Building Physics Laboratory, Civil Engineering Department Faculty of Engineering, University of Porto, Porto, Portugal
e-mail: jdelgado@fe.up.pt

V. A. B. de Oliveira
Department of Civil Engineering, State University of Paraíba, Araruna, PB, Brazil
e-mail: vitaloliveira@uepb.edu.br

J. M. P. Q. Delgado and A. G. Barbosa de Lima (eds.), *Transport Phenomena and Drying of Solids and Particulate Materials*, Advanced Structured Materials 48,
DOI: 10.1007/978-3-319-04054-7_1,

1 Introduction

The diffusion phenomenon occurs in many industrial processes, such as drying, wetting, heating and cooling. These processes have been applied to preservation and conservation of different biological products, mainly foodstuffs (grains, fruits, vegetables, etc.) well known as hygroscopic capillary-porous bodies.

Drying is one of the most important processes used in the processing of foods and in the storage of grains. This process consists of the partial transfer of the liquid part (usually water) of a wet solid. The drying process can also be explained as a process of heat and mass transfer that generates the removal through evaporation of part of the moisture contained in the product [1] and takes place simultaneously with geometrical variations (shrinkage, dilation and deformation) and physical and micro-structural modifications (color, flavour, appearance, nutrients, germination, depending on the product species). Drying differs from other separation techniques due to the movement of the molecules, which in this case is obtained by a mass transfer of the liquid and/or vapor due to the difference in partial pressure of the steam between the surface of the solid to be evaporated and the air that surrounds it. In the case of foods, water must be removed from the moist material up to a level where deterioration provoked by microorganisms can be minimised, in order to maintain quality characteristics these products that determine its acceptance and commercialization. However, drying rate is affected by many factors such as velocity, temperature and relative humidity of air, type of solid and dryer, drying method and initial moisture content of solid.

For accurately describe moisture migration within biological products, mainly foodstuffs (grains, fruits, vegetables, etc.) and to explain the effects of drying on the quality of the material, the heat and moisture transfer within a individual particles must be understood and accurately represented by a mathematical model. From a review of the literature, it is noted that several researches prefer the diffusion model applied only to known geometric shapes specifically: plates, cylinders, spheres and parallelepipeds [2–5], and for prolate and oblate spheroidal bodies [6–14] with specified boundary conditions and constant thermo-physical properties assuming moisture migration inside the solid by liquid or vapor diffusion only. However, other researchers shown that the moisture migrates in both liquid and vapor phases can occur within the solid, due to concentration gradients, partial vapor-pressure gradients, capillary forces, differences in total pressure and gravity [1, 15–27].

According to Luikov [19], transfer of vapor and inert gas can take place by molecular means in the form of diffusion and by molar means due to filtration motion of the whole steam-gas mixture within the porous body under the influence of a fall in aggregate pressure. Therefore, the derivation of a model of mass transfer in capillary-porous bodies on the basis of molecular and molar transfer mechanism presents great difficulties. In this sense, Fortes [1], Fortes and Okos [24], Fortes et al. [28] present a set of transport equations that incorporates most of the models presented in the literature by combining the mechanistic and irreversible thermodynamics approaches to describe heat and mass transfer in porous media. In the model is postulated to be valid the Gibb's equation, linear phenomenological laws, Onsager's fundamental theorem, Curie's principle and local thermodynamic equilibrium. Based on the thermodynamic concept only, the authors has proposed that the driving-force for moisture migration in the liquid and vapor phases is the local equilibrium moisture content gradient instead of the moisture content as reported in the literature (Fick's second law of diffusion). Thus, water may migrates from region of lower to higher moisture content, since the region of higher moisture content is at a lower equilibrium moisture content and the temperature gradient term is greater than the equilibrium moisture content gradient term and favors this movement. Under isothermal condition, water always moves from regions of higher to lower equilibrium moisture content. As related by Fortes and Okos [24] all the physical parameters cited in the model can be obtained from experimental techniques.

How complement for these researches, in this chapter, a two-dimensional numerical analysis is performed for simultaneous heat and mass (liquid and vapor) transport in bodies with ellipsoidal shape, using the Fortes and Oko's theory (non-equilibrium thermodynamic approaches).

2 The Macroscopic Governing Equation

2.1 General Distributed Model

In the model which will be presented here, the following considerations were made:

(a) The solid is considered to be homogeneous and continuum;
(b) The shape of solid is approached to be an ellipsoid of revolution;
(c) The body is axially symmetric around z-axis;
(d) The solid is composed of water in liquid and vapor phases and solid matter;
(e) The shrinkage and dilation are neglected;
(f) The unique mechanism of drying is diffusion;
(g) Convection phenomenon within the solid is negligible.
(h) Moisture migration (liquid and vapor) due to gravity is negligible;
(i) The liquid and vapor diffusion phenomenon occurs under falling drying rate;
(j) Thermo-physical properties are variables during drying process;
(k) The moisture content and temperature fields are considered symmetric around z-axis at any time and constant in the beginning of the process;
(l) The phenomenon occurs under equilibrium or convective boundary condition at the surface;
(m) No energy and mass generation occurs within the solid.

2.1.1 Mass Diffusion Model

The moisture transport within the solid was assumed to be in the liquid and vapor states and governed by the transient liquid and vapor diffusion equation. For the model of mass transfer inside the wet porous solid we have the following equations [1, 24, 27, 28]:

- Liquid flux:

$$\vec{J}_\ell = -\rho_\ell k_\ell R_v \ell n H \nabla T - \rho_\ell k_\ell \frac{R_v T}{H}\frac{\partial H}{\partial M}\nabla M + \rho_\ell k_\ell \vec{g} \tag{1}$$

- Vapor flux:

$$\vec{J}_v = -k_v\left(\rho_{vo}\frac{\partial H}{\partial T} + H\frac{d\rho_{vo}}{dT}\right)\nabla T - k_v\rho_{vo}\frac{\partial H}{\partial M}\nabla M + \left(\frac{Hk_v\rho_{vo}}{TR_v}\right)\vec{g} \tag{2}$$

where M (dry basis) should be taken as the equilibrium moisture content in any location inside the porous media. In this equations $\vec{g}$ is the gravitational acceleration vector; H is the relative humidity; k_l is the liquid conductivity; k_v is the vapor conductivity; R_V is the universal gas constant as applied to air; T is the air temperature; q is the density.

Assuming that no ice is present, that the mass of air is neglected, and that mass of vapor is neglected in comparison with the mass of liquid (but not its flux) [19], one mass balance in an differential control volume leads to:

$$\frac{\partial(\rho_s M)}{\partial t} = -\nabla \cdot \left(\vec{J}_\ell + \vec{J}_v\right). \tag{3}$$

2.1.2 Heat Conduction Model

For the model of heat transfer inside the wet porous solid, we have the following energy equation [1, 24, 27, 28]:

$$\frac{\partial}{\partial t}(\rho_s c_b T) - \frac{\partial}{\partial t}(\rho_s L_w M) = -\nabla \cdot \vec{J}_q - \nabla \cdot \left(L_v \vec{J}_v\right) - \vec{J}_\ell \cdot c_\ell \nabla T - \vec{J}_v \cdot c_v \nabla T \tag{4}$$

where the c is the specific heat; L_w is the specific differential heat of wetting and L_v is the specific latent heat of vaporization. The heat flux is given by:

$$\begin{aligned}\vec{J}_q = & -k_T\nabla T - \left[\rho_\ell k_\ell R_v \ell n H + k_v\left(\rho_{vo}\frac{\partial H}{\partial T} + H\frac{d\rho_{vo}}{dT}\right)\right]\frac{R_v T^2}{H}\frac{\partial H}{\partial M}\nabla M \\ & + T\left[\rho_\ell k_\ell R_v \ell n H + k_v\left(\rho_{vo}\frac{\partial H}{\partial T} + H\frac{d\rho_{vo}}{dT}\right)\right]\vec{g}\end{aligned} \tag{5}$$

where k_T is the thermal conductivity. More details about the notation may be found in the references cited in the text.

2.2 Conservation Equations Applied to Prolate Spheroidal Solids

For better understanding of the problem treated herein, we must consider the diffusion phenomenon in an ellipsoid of revolution, in which the axis of revolution is greater than the other axis as pictured in Fig. 1. In this case it is said to be prolate spheroid, while, if the axis of revolution is smaller than the other, it is called oblate spheroid. Further, if the axis of revolution is equal to the other axis, the solid is called sphere.

Based in the shape of the solid to be studied (Fig. 1), is better to use a new orthogonal coordinate system ξ, η, ζ instead of the Cartesian coordinate x, y and z. In the case of the body with ellipsoidal geometric shape, an adequate coordinate system is the prolate spheroidal coordinate system (Fig. 2). The mathematical relations between Cartesian and prolate spheroidal coordinate systems are given by [29–31]:

$$x = L\sqrt{(1-\xi^2)(\eta^2-1)\zeta} \tag{6}$$

$$y = L\sqrt{(1-\xi^2)(\eta^2-1)}\sqrt{(1-\zeta^2)} \tag{7}$$

$$z = \mathrm{L}\,\xi\,\eta \tag{8}$$

where $\xi = \cosh\mu$; $\eta = \cos\phi$; $\zeta = \cos\omega$ and $L = (L_2^2 - L_1^2)^{1/2}$ is the focal length.

According to Fig. 2, the surfaces $\xi = \xi_o$ (constant), $\xi_o > 1$ is an elongated ellipsoid of revolution with major axis of length $L\xi$ and minor axis of length $L(\xi^2 - 1)^{1/2}$. The surfaces ξ constant are a confocal family of prolate spheroids having their common center at the origin. The degenerate surface $\xi = 1$ is the curve that link the center ($z = 0$) to the focal point ($z = L$). The surface $\eta = \eta_o$ (constant), $\eta_o < 1$, is a hyperboloid of revolution of two sheets with an asymptotic cone whose generating by line passes through the origin and is inclined at the angle $\phi = \cos^{-1}\eta$ to the z-axis. The degenerate surface $\eta = 1$ is part of the axis $z > L$.

Then, calculating the metric coefficients of the transformation of coordinates, the volume of the body, the gradient and the Laplacian for the new coordinate system, utilizing the symmetry around the z-axis, $\partial/\partial\omega = 0 \Rightarrow \partial/\partial\zeta = 0$ and using the considerations presented, the governing mathematical equations can be formulated in the prolate spheroidal coordinate system [6, 8, 9, 15–17, 29].

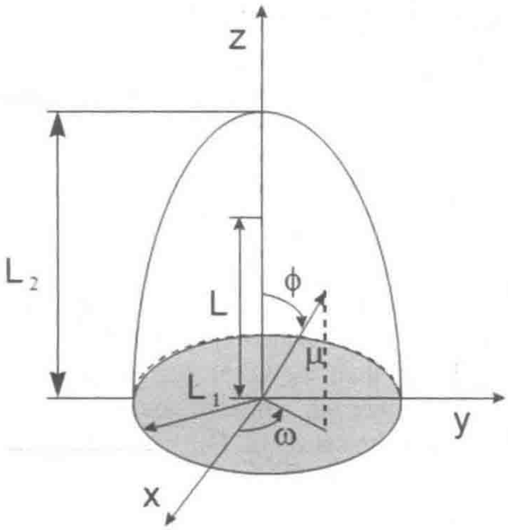

Fig. 1 Geometrical parameters and shape of a prolate spheroidal solid

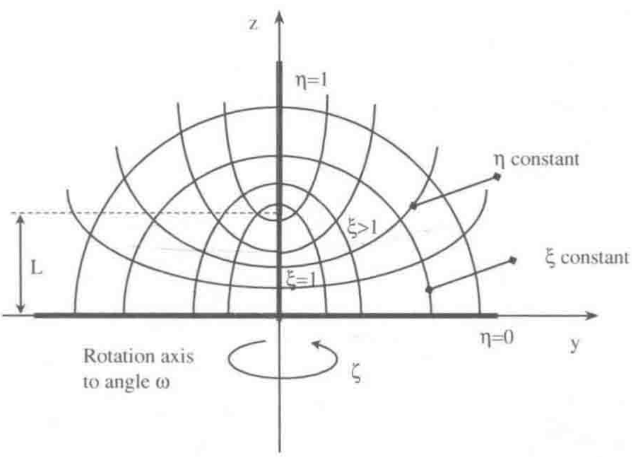

Fig. 2 Prolate spheroidal coordinate system

The mass transfer equation, Eq. (3), written in prolate spheroidal coordinates is:

$$\begin{aligned}\frac{\partial(\rho_s M)}{\partial t} &= \frac{1}{L^2(\xi^2-\eta^2)}\left\{\frac{\partial}{\partial \xi}\left[(\xi^2-1)\Gamma_1^{\Phi}\frac{\partial M}{\partial \xi}\right]+\frac{\partial}{\partial \eta}\left[(1-\eta^2)\Gamma_1^{\Phi}\frac{\partial M}{\partial \eta}\right]\right\}\\ &+\frac{1}{L^2(\xi^2-\eta^2)}\left\{\frac{\partial}{\partial \xi}\left[(\xi^2-1)\Gamma_2^{\Phi}\frac{\partial T}{\partial \xi}\right]+\frac{\partial}{\partial \eta}\left[(1-\eta^2)\Gamma_2^{\Phi}\frac{\partial T}{\partial \eta}\right]\right\}\end{aligned} \tag{9}$$

where

$$\Gamma_1^{\varphi} = \left(\rho_\ell k_\ell \frac{R_v T}{H}\left(\frac{\partial H}{\partial M}\right) + k_v \rho_{v0}\left(\frac{\partial H}{\partial M}\right)\right); \tag{10}$$

$$\Gamma_2^{\varphi} = \left(\rho_\ell k_\ell R_v \ln(H) + k_v\left(\rho_{v0}\frac{\partial H}{\partial T} + H\frac{d\rho_{v0}}{dT}\right)\right); \tag{11}$$

To complete the mathematical formulation, the following initial and boundary conditions are used:

- Free surface: the mass diffusive flux is equal to the mass convective flux at the surface of the solid.

$$\left(\vec{J}_\ell + \vec{J}_v\right)\Big|_{\xi=\xi_f} = h_m\left(M_{\xi=\xi_f} - M_e\right) \tag{12}$$

where $n_f = L_2/L$ at the surface

- Planes of symmetry: the angular and radial gradients of moisture content are equals to zero at the planes of symmetry.

$$\frac{\partial M(\xi;\quad \eta = 1;\quad t)}{\partial \eta} = 0 \tag{13}$$

$$\frac{\partial M(\xi;\quad \eta = 0;\quad t)}{\partial \eta} = 0 \tag{14}$$

$$\frac{\partial M(\xi = 1;\quad \eta;\quad t)}{\partial \xi} = 0 \tag{15}$$

- Initial condition in the interior of the solid

$$M(\xi;\quad \eta;\quad t = 0) = M_o \tag{16}$$

The average moisture content of the body at any instant was calculated as follows:

$$\overline{M} = \frac{1}{V}\int_V M dV \tag{17}$$

where V is the volume of the ellipsoidal body calculated as follows:

$$V = \frac{4}{3}\pi L_2 L_1^2 \tag{18}$$

The energy equation, Eq. (4), written in prolate spheroidal coordinates is:

$$
\begin{aligned}
\frac{\partial}{\partial t}(\rho_s c_b T) - \frac{\partial}{\partial t}(\rho_s L_w M) = {} & \frac{1}{L^2(\xi^2-\eta^2)}\left\{\frac{\partial}{\partial \xi}\left[(\xi^2-1)\Gamma_3^{\Phi}\frac{\partial T}{\partial \xi}\right] + \frac{\partial}{\partial \eta}\left[(1-\eta^2)\Gamma_3^{\Phi}\frac{\partial T}{\partial \eta}\right]\right\} \\
& + \frac{1}{L^2(\xi^2-\eta^2)}\left\{\frac{\partial}{\partial \xi}\left[(\xi^2-1)\Gamma_5^{\Phi}\frac{\partial T}{\partial \xi}\right] + \frac{\partial}{\partial \eta}\left[(1-\eta^2)\Gamma_5^{\Phi}\frac{\partial T}{\partial \eta}\right]\right. \\
& \left. + \frac{\partial}{\partial \xi}\left[(\xi^2-1)\Gamma_4^{\Phi}\frac{\partial M}{\partial \xi}\right]\right\} + \frac{1}{L^2(\xi^2-\eta^2)} \\
& \left\{+\frac{\partial}{\partial \eta}\left[(1-\eta^2)\Gamma_4^{\Phi}\frac{\partial M}{\partial \eta}\right] + \frac{\partial}{\partial \xi}\left[(\xi^2-1)\Gamma_6^{\Phi}\frac{\partial M}{\partial \xi}\right] + \frac{\partial}{\partial \eta}\left[(1-\eta^2)\Gamma_6^{\Phi}\frac{\partial M}{\partial \eta}\right]\right\} \\
& + \frac{\Gamma_7^{\Phi}}{L^2(\xi^2-\eta^2)}\left[(\xi^2-1)\left(\frac{\partial T}{\partial \xi}\right)^2 + (1-\eta^2)\left(\frac{\partial T}{\partial \eta}\right)^2\right] \\
& + \frac{\Gamma_8^{\Phi}}{L^2(\xi^2-\eta^2)}\left[(\xi^2-1)^2\frac{\partial T}{\partial \xi}\frac{\partial M}{\partial \xi} + (1-\eta^2)\frac{\partial T}{\partial \eta}\frac{\partial M}{\partial \eta}\right]
\end{aligned}
\tag{19}
$$

where

$$\Gamma_3^{\Phi} = k_T; \tag{20}$$

$$\Gamma_4^{\Phi} = \left[\rho_\ell k_\ell R_v \ell n(H) + k_v\left(\rho_{v0}\frac{\partial H}{\partial T} + H\frac{d\rho_{v0}}{dT}\right)\right]\left(\frac{R_v T^2}{H}\frac{\partial H}{\partial M}\right); \tag{21}$$

$$\Gamma_5^{\Phi} = L_v k_v\left(\rho_{v0}\frac{\partial H}{\partial T} + H\frac{d\rho_{v0}}{dT}\right); \tag{22}$$

$$\Gamma_6^{\Phi} = L_v k_v \rho_{v0}\left(\frac{\partial H}{\partial M}\right); \tag{23}$$

$$\Gamma_7^{\Phi} = c_\ell \rho_\ell k_\ell R_v \ell n(H) + k_v c_v\left(\rho_{v0}\frac{\partial H}{\partial T} + H\left(\frac{d\rho_{v0}}{dT}\right)\right); \tag{24}$$

$$\Gamma_8^{\Phi} = c_\ell \rho_\ell k_\ell \frac{R_v}{H}\left(\frac{\partial H}{\partial M}\right) + k_v c_v \rho_{v0}\frac{\partial H}{\partial M}. \tag{25}$$

The initial and boundary conditions are:

- Free surface: the heat convective flux supplied to the body surface equals to the heat diffusive flux plus the energy necessary to evaporate the liquid water and to heat the vapor produced at the surface of the prolate spheroid from surface temperature to the drying-air temperature.

$$\vec{J}_q\Big|_{\xi=\xi_f} = h_c\left(T_a - T_{\xi=\xi_f}\right) + L_v\vec{J}_\ell + (\vec{J}_\ell + \vec{J}_v)c_v\left(T_a - T_{\xi=\xi_f}\right) \tag{26}$$

- Planes of symmetry: the angular and radial gradients of temperature are equals to zero at the planes of symmetry.

$$\frac{\partial T(\xi; \quad \eta = 1; \quad t)}{\partial \eta} = 0 \tag{27}$$

$$\frac{\partial T(\xi; \quad \eta = 0; \quad t)}{\partial \eta} = 0 \tag{28}$$

$$\frac{\partial T(\xi = 1; \quad \eta; \quad t)}{\partial \xi} = 0 \tag{29}$$

- Initial condition inside the solid

$$T(\xi; \quad \eta; \quad t = 0) = T_0 = cte \tag{30}$$

The average temperature of the body during diffusion phenomenon was calculated as follows:

$$\bar{T} = \frac{1}{V} \int_V T dV \tag{31}$$

This heat and mass transfer model is interesting and complex because it incorporates the mechanistic [32–35] and the irreversible thermodynamic approaches [18, 19, 21, 36, 37]. More details about the heat and mass transfer model reported here may be found in Fortes [1], Fortes et al. [28] and Oliveira [38].

3 Computational Strategy for Solution of the Governing Equations and Simulation

Various numerical methods have been used to solve the problem of transient diffusion, such as, finite-difference, finite-element, boundary-element and finite-volume methods. Several discussions may be encountered in previous reports [39–42]. In particular, in this work, we used the finite-volume method. In the simulation of diffusion phenomenon in prolate spheroids was utilized a certain domain, due to the symmetry of the body. Assuming fully implicit formulation, the Eqs. (9) and (17) were integrated in the volume and time. How results the following discretization equation was obtained:

$$A_P \Phi_P = A_E \Phi_E + A_W \Phi_W + A_N \Phi_N + A_S \Phi_S + A_P^o \Phi_P^o + B \tag{32}$$

where Φ represents M or T and B is the source term. Details about the discretization procedure can be found in the references cited in the text.

Equation (32) constitutes a set of linear algebraic equation which must be solved, in order for obtain the kinetic values and distribution of the potential Φ inside the solid at any instant. The method employed to solve it was the Gauss-Siedel iterative method. Convergence was assumed to have been reached when the following absolute value is obtained in all nodal points:

$$\left|\Phi^{k+1} - \Phi^{k}\right| \leq 10^{-8} \tag{33}$$

where Φ represents M or T and k represent kth iteration.

In the discretization, the interface properties and non linearity (source-term linearization) were treated according to Patankar [40] and Maliska [41]. A computational code utilizing the Mathematica® commercial software was written to solve the set of equations for the moisture content and temperature profile and to determine the average moisture content and temperature.

The application of the finite-volume numerical method is seriously affected by the Δt values and the number of grid points utilized in the numerical calculations. In order to verify grid size and time step independence, results were obtained with four grid sizes and time steps. After this study, it was chosen a mesh with 20×20 nodal points and $\Delta t = 1$ s to be used in the iterative scheme. Figure 3 shows the numerical grid generated.

According to Lima and Nebra [6], for prolate spheroids, the shape of the mesh varies with L_2/L_1. When $L_2/L_1 \to \infty$, the focal point is dislocated to the surface of the body; the inverse occurs for $L_2/L_1 \to 1$, when the focal point tends to coincide with the geometrical center of the body. On the zy plane (physical plane), the control volumes are not uniformly spaced, presenting a higher concentration near the surface of the body relative to ξ (radial coordinate), and on the y axis relative to η (angular coordinate). Then, an irregular grid is obtained; however, in the $\xi\eta$ plane (computational plane), we have a regular grid. This regular grid has the property that the ratio of lengths of any two adjacent intervals is a constant and equal to one. Just in this plane all the numerical calculations are performed.

In the numerical stability analysis performed, only the finite-volume approach inside the solid was considered, and we does not have mechanisms to predict the influence of the boundary conditions on the numerical stability. The boundary values have large influence on grid spacing only at the nodal points immediately near the surface of the body, in spite of the elliptic character of Eqs. (9) and (19).

4 Application

4.1 Physical Problem Description: Wheat Grain Drying

Several biological products has shape approximately ellipsoidal, in the particular case, prolate spheroidal. As examples, we can cite rice, wheat, orange, silkworm cocoon and banana. The problem of heat and mass transfer in a prolate spheroid it

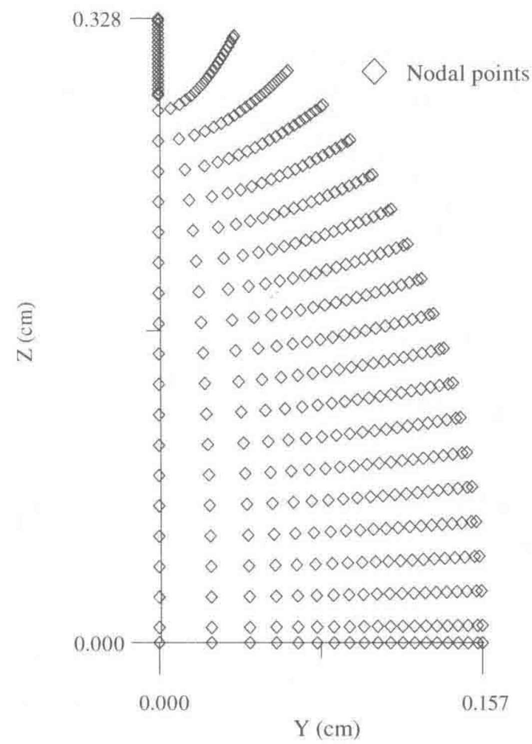

Fig. 3 Numerical grid in the physical plane

is of great interest because, it represents a high degree of precision of the problem in comparison to the approach this problem for cases of sphere or cylinder as used today. Since that sphere and cylinder are particular cases of prolate spheroids, it is now unnecessary to repeat the complex derivation for each different geometric shape.

Grain drying and storage are of great importance to the agricultural industry. Each year large quantities of grains are dried and placed in storage. The removal of moisture from agricultural crops has been subject of considerable research.

Wheat is a cereal crop produced worldwide; today it is grown all over the world, with different varieties shown according to the various climates.

Globally, wheat is an important human energy source and is one of the major staple foods because of its agronomical adaptability, ability of its flour to be made into various food material and ease of storage [43]. Wheat grain must be dried to 13.5 percent for immediate sale since over drying reduces the total weight of grain to be sold. However, if wheat is to be stored for any period of time, it is dried to 12 to 12.5 percent moisture content to prevent spoilage.

Wheat production is a direct function of high yielding varieties, chemical, fertilizers, mechanization and other energy inputs [44]. In Brazil, the average annual production of wheat in 2011 comes to about 5.69 million tones, against World's average of 701.40 million tones in the same year. Thus, Brazil presents a reduced contribution to the World wheat production. In the year 2011, the area under wheat cultivation in Brazil, comes to about 2.17 million ha which is many reduced in comparison with the World's wheat area [45].